Design and optimization of the secondary circuit for the WCLL BB option of the EU-DEMO power plant

Leszek Malinowski[a], Monika Lewandowska[a], Fabio Giannetti[b]

[a]West Pomeranian University of Technology, Szczecin, Al. Piastów 17, 70-310 Szczecin, Poland
[b] Sapienza University of Rome, DIAEE Nuclear Section, Rome, Italy

EU-DEMO will be a DEMOnstration Fusion power plant designed to demonstrate production of grid electricity from fusion at the level of a few hundred MW. The Primary Heat Transfer System (PHTS) transfers heat from the breeding blanket (BB), divertor and vacuum vessel to the secondary Power Conversion System (PCS) responsible for conversion of thermal energy into electricity. Two main BB conceptions, and the relative PHTSs, for EU-DEMO are being developed: the Helium Cooled Pebble Bed (HCPB) BB and the Water Cooled Lithium Lead (WCLL) BB. Two options for each conception are considered: with or without the Intermediate Heat Transfer System (IHTS), containing the Energy Storage System (ESS), between the BB PHTS and PCS. The role of IHTS+ ESS is to ensure continuous smooth thermal energy transfer from the reactor sources to PCS despite the pulsed operation of the DEMO reactor. In the present work we discuss the mature concept of the PCS configuration for the option WCLL BB with the IHTS+ESS (based on the 2018 EU-DEMO reference), which allows almost constant production of electricity during both plasma pulse and dwell phases. The operating parameters of the circuit were optimized to minimize the temperature oscillations $\Delta T = |T_{pulse} - T_{dwell}|$ in all the circuit components, which occur due to the pulsation of the DEMO cold sources of Divertor and Vacuum Vessel whose HXs are integrated in PCS itself. Operation of the PCS circuit during the pulse and dwell phases was simulated using the GateCycle software, to show the system performance and to enable discussion on the feasibility of the concept.

Keywords: EU-DEMO, Power Conversion System, Water Cooled Lithium Lead Bed Breeding Blanket, Energy Storage System, GateCycle

1. Introduction

The EU-DEMO (DEMOnstration Fusion power plant) is being designed in the frame of the European Fusion Programme (EUROfusion) to start operation by about 2060 [1-4]. The main objectives of DEMO are: achieving a long plasma operation time ($\geq$ 2 h), production of net electricity output at a level of several hundred MW, ensuring tritium self-sufficiency, achieving reasonable availability up to several full-power years, and limitation of radioactive wastes including also avoidance of long-term storage [5,6].

The Primary Heat Transfer System (PHTS) of the EU DEMO plant transfers thermal power from the tokamak heat sources, which include: Breeding Blanket (BB), Divertor (DIV) and the Vacuum Vessel (VV), to the secondary Power Conversion System (PCS). The role of the PCS is conversion of heat into mechanical energy due to the steam expansion in the turbines, and then such shaft mechanical power is used for generation of electricity in the synchronous generator. Two main concepts for the EU DEMO BB and the respective PHTS are developed, i.e. the Helium-Cooled Pebble Bed BB [7,8], and the Water Cooled Lithium Lead (WCLL) BB [9,10].

One of the main concerns of EU DEMO BoP designers is pulsed operation of the tokamak. According to the current EU DEMO operation scenario, 120 min long plasma burn pulses will be separated by about 10 min long dwell periods [2]. This implies very large oscillations of thermal power production in the DEMO reactor (100% nominal power during pulse and only ~1% of nominal power during dwell) occurring frequently (~11 times per day). To mitigate the respective transients and their negative effects on turbine operation and lifetime of the PCS components, in some DEMO plant configurations an Intermediate Heat Transfer System (IHTS) with the Energy Storage System (ESS) filled with HITEC Molten Salt (MS), has been integrated between the PHTS and PCS [5,9,11]. However, adding IHTS / ESS increases complication and cost the plant design, so in parallel other options with more direct coupling of the PHTS with the PCS are also being considered [5,12,13].

In the present study we discuss the detailed GateCycle (GC) model of the fully mature design of steam/water PCS for the option WCLL BB with the IHTS+ESS, which was developed as a continuation of our efforts presented in [14-16]. Operation of the PCS during the plasma pulse and during the dwell phase is analyzed and the operating parameters of the cycle are optimized to minimize the temperature oscillations $\Delta T = |T_{pulse} - T_{dwell}|$ in all the circuit components.

2. Basic assumptions

2.1. Characteristics of the DEMO heat sources

The updated concept of the EU-DEMO plant configuration for the option WCLL BB with the IHTS+ESS, based on the 2018 DEMO reference, was

proposed by its designers in [17,18]. The proposed PCS utilizes heat taken from the following reactor sources: BB cooled with two separate cooling circuits (one for the blanket First Wall (FW) and one for the Breeding Zone (BZ)), Divertor (DIV) also cooled with two separate circuits (one for the Plasma Facing Components (PFC) and one for the Cassette (CAS)), and Vacuum Vessel (VV). The operational parameters of the reactor heat sources are reported in Table 1. Heat from the BB BZ is utilized to produce steam in the Once Through Steam Generator (OTSG), whereas heat extracted from VV and from DIV is used to preheat feed water in the respective heat exchangers (HXs). During the pulse phase (2 h) the BB FW PHTS power (439.8 MW$_{th}$) is provided to the ESS. Part of this energy (~266 MW) is directly delivered to PCS via one Helical Coil Steam Generator (HCSG). The remaining part (~174 MW) is accumulated in the ESS. The energy stored during the pulse phase, equal to ~1.25×10^6 MJ, is then provided to the PCS during the dwell phase, and is utilized to produce steam in the HCSG. During the dwell, the HCSGs are designed to remove 521 MW for each component. Instead, during pulse mode, only one of the four HCSGs is active and it works at 51% of the nominal power, maintaining an acceptable load to avoid possible two-phase instabilities. The main parameters of the HCSG, in pulse and dwell mode are compiled in Table 2.

In the dwell period most of heat is provided to the circuit from the ESS via HCSG, whereas thermal power of all the reactor sources drops to the level of their decay heat (1% of the nominal value for each source). In order to compensate the power reduction during dwell of the heat exchangers DIV PFC, VV and DIV CAS, three additional HXs, namely: FWH_DW1, FWH_DW2 and FWH_DW3, respectively, fed with live steam have been integrated in PCS.

2.2 GateCycle model

In the present study we developed a detailed GC model of the PCS circuit proposed in [17,18] and optimized its operating parameters. At the first stage of our analysis, focused on the preliminary design and sizing of the main circuit components, the convergent GC model (in the "Design" mode) of the whole PCS circuit for the PULSE phase was created [19]. We designed separately the HCSG and the HXs FWH_DW1, FWH_DW2 and FWH_DW3. These devices were then added to the GC model of the PCS circuit as "Off design" components (i.e. with the fixed design). Layout of our GC PCS model is presented in Fig. 1. It should also be mentioned, that GC does not support molten salt as a working fluid. To overcome this limitation we replaced the original HCSG used in [17,18] with a steam generator (MS HCSG in Fig. 1) in which the equivalent amount of thermal power at the hot side was provided by steam. Thus, the heat transfer area of the steam generator MS HCSG computed with our model is incomparable with the heat transfer area of the corresponding actual MS/water heat exchanger.

In the second stage of our analysis a large number of "Off-design" cases of this GC model were simulated, in which the thermal power of heat sources and the values of operational parameters were modified gradually till they eventually reached the state corresponding to the dwell phase, which was close to that specified in [17,18]. These "Off design" simulations served as verification of the potential operational feasibility of the considered PCS circuit.

The last stage of our analysis was focused on optimization (in the "Off design" mode) of the operating parameters of the considered PCS circuit, aimed at minimization of the temperature oscillations $\Delta T = |T_{pulse} - T_{dwell}|$ in all the circuit components. These temperature fluctuations, which may occur due to the power pulsation of the DEMO cold sources (Divertor and Vacuum Vessel), are very undesirable, since they may cause excessive thermal stresses and shorten the life time of PCS components due to the thermal fatigue.

The "Design" calculations of turbines were made using the Spencer Cotton Cannon efficiency method with the input extraction pressures, whereas for the "Off-design" calculations the Spencer Cotton Cannon efficiency method and the modified Stodola extraction pressure method were used. We assumed that the heat losses in heat HXs are equal to 1% of the heat rate provided to the cold fluid. We took into account pressure drop in heat exchangers and along the pipes. For the deaerator we assumed operation at constant pressure with pegging control of the main steam flow.

2.3 PCS description

As shown in Fig. 1, the superheated steam flows to the high pressure (HP) turbine (consisting of 3 stages). After exiting the HP turbine the expanded steam is drained in the moisture separator (MSEP1), and hereafter superheated in the reheater (HX_REHEAT) before entering the low pressure (LP) turbine (3 stages). The 50 mbar steam leaving the LP turbine is condensed in the condenser (CND1), hereafter the condensate is pumped successively into the LP feedwater heaters FWH-1 and FWH-2, where it is pre-heated using the steam extracted from the 2nd and 1st stage of the LP turbine, respectively. Then the feedwater, further pre-heated in the HXs DIV_PFC and FWH_DW1 connected in parallel, arrives to the deaerator (DA1) fed by the steam extracted from the 3rd stage of the HP turbine. Then the feedwater is pumped by the main circulation pump (PUMP-2) from DA1 via the HP heat exchangers: VV (connected in parallel with FWH_DW2), DIV-CAS (connected in parallel with FWH_DW3), FWH to the inlet of the steam generators OTSG and HCSG connected in parallel.

2.4 Power and efficiency calculations

The gross power produced by the generator (W_{gross}) was defined as in our earlier studies [12,15,16], namely:

$$W_{gross} = \eta_{gen}(W_{t1} + W_{t2}),\qquad(1)$$

where $\eta_{gen} = 0.98$ is the assumed generator efficiency and W_{ti} is the shaft power of the i-th turbine ($i = 1, 2$). The net mechanical power produced by the considered Rankine power cycle (W_{cycle}) was defined as:

$$W_{cycle} = \sum_{i=1}^{2} W_{t_i} - \sum_{i=1}^{5} W_{Rankine\ pump_i} , \qquad (2)$$
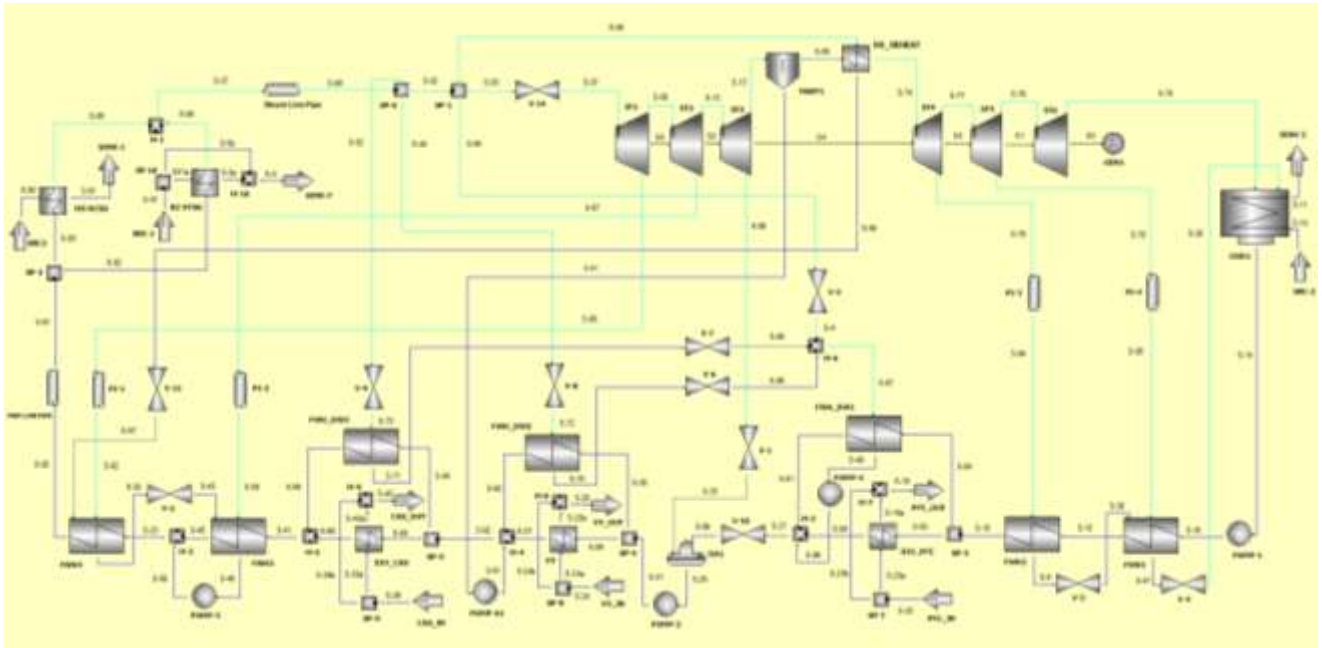

Fig. 1. Scheme of the considered PCS circuit.

Table 1. Characteristics of the heat sources in the EU DEMO PHTS for the option WCLL BB [17,18].

Source	BB FW	BB BZ	DIV CAS	DIV PFC	VV
Coolant	water	water	water	water	water
Thermal power pulse/dwell (MW)	439.8 / 4.40	1483 /14.83	115.2 / 1.15	136 / 1.36	86 / 0.86
Mass flow rate pulse/dwell (kg/s)	2272 / 2272	7660 / 7660	860.8 / 860.8	5318 / 5318	1928 / 1928
Outlet temperature pulse/dwell (ºC)	328 / 312	328 / 312	210 / 195	136 / 133	200 / 195
Inlet temperature pulse/dwell (ºC)	295 / 312	295 / 312	180 / 195	130 / 133	190 /195
Operating pressure (MPa)	15.5	15.5	3.5	3.8	3.15

Table 2. Characteristics of the MS HCSG during the pulse and dwell phases [17,18]

Description	PULSE	DWELL
No. operating HCSG	1 (3 off)	4
Operation power pulse/dwell (MW$_{th}$)	266	521.6 (x 4)
HITEC inlet temperature pulse/dwell (ºC)	320	320
HITEC outlet temperature pulse/dwell (ºC)	280	280
HITEC mass flow rate pulse/dwell (kg/s)	4266	8345 (x 4)
Liquid water inlet temperature pulse/dwell (ºC)	238	238
Steam outlet temperature pulse/dwell (ºC)	299	299
Water mass flow rate pulse/dwell (kg/s)	145	284 (x 4)

Table 3. Characteristics of the selected streams during the plasma pulse and during the dwell period.

Stream	From	To	PULSE				DWELL			
			$\dot{m}$ (kg/s)	p (MPa)	T (ºC)	quality	$\dot{m}$ (kg/s)	p (MPa)	T (ºC)	quality
S-0	M-10	SINK-7	7660.0	15.500	294.6	0	7660.0	15.500	311.7	0
S-01	SRC-1	SP-10	7660.0	15.500	328.0	0	7660.0	15.500	312.0	0
S01a	SP-10	BZ OTSG	7277.0	15.500	328.0	0	87.7	15.500	312.0	0
S-02	SP-6	SP-1	958.4	6.381	296.2	1	1053.5	6.598	297.4	1

S-03	SP-1	V-14	863.5	6.381	296.2	1	896.1	6.598	297.4	1
S-05	MSEP1	HX_REHEAT	708.4	1.100	184.1	0.991	701.5	1.091	183.7	0.991
S-06	SP-1	HX_REHEAT	92.8	6.381	296.2	1	103.0	6.598	297.4	1
S-07	V-14	ST1	863.5	6.381	296.2	1	896.1	6.598	297.4	1
S-0a	BZ OTSG	M-10	7277.0	15.500	292.7	0	87.7	15.500	280.4	0
S-0b	SP-10	M-10	383.0	15.500	328.0	0	7572.3	15.500	312.0	0
S-13	ST3	MSEP1	789.4	1.100	184.1	0.889	786.7	1.091	183.7	0.884
S-14	CND1	PUMP-1	708.4	0.005	31.9	0	701.5	0.005	31.9	0
S-15	FWH1	FWH2	708.4	0.595	66.2	0	701.5	0.597	65.1	0
S-16	PUMP-1	FWH1	708.4	0.680	32.0	0	701.5	0.680	31.9	0
S-18	FWH2	SP-3	708.4	0.528	89.0	0	701.5	0.531	87.9	0
S-19	M-7	PFC_OUT	5317.9	3.800	129.9	0	5317.9	3.800	132.9	0
S-19a	DIV_PFC	M-7	5291.3	3.800	129.9	0	37.0	3.800	124.3	0
S-20	PFC_IN	SP-7	5317.9	3.800	136.0	0	5317.9	3.800	133.0	0
S-20a	SP-7	DIV_PFC	5291.3	3.800	136.0	0	37.0	3.800	133.0	0
S-20b	SP-7	M-7	26.6	3.800	136.0	0	5280.9	3.800	133.0	0
S-21	M-2	V-10	711.6	0.457	135.9	0	846.6	0.444	135.8	0
S-23	M-3	FWH4	959.5	6.780	219.2	0	1144.1	7.096	215.1	0
S-24	VV_IN	SP-8	1928.0	3.150	200.0	0	1928.0	3.150	195.0	0
S-24a	SP-8	VV	1922.2	3.150	200.0	0	13.4	3.150	195.0	0
S-24b	SP-8	M-8	5.8	3.150	200.0	0	1914.6	3.150	195.0	0
S-25	DA1	PUMP-2	716.2	0.350	138.9	0	854.0	0.360	139.9	0
S-26	M-8	VV_OUT	1928.0	3.150	189.9	0	1928.0	3.150	194.9	0
S-26a	VV	M-8	1922.2	3.150	189.9	0	13.4	3.150	180.4	0
S-27	VV	M-4	710.9	7.178	168.0	0	4.5	7.615	184.9	0
S-28	FWH4	FWH LINE PIPE	959.5	6.631	238.5	0	1144.1	6.905	237.7	0
S-29	V-4	CND1	73.1	0.005	32.0	0	70.9	0.005	31.9	0
S-31	PUMP-2	SP-4	716.2	7.269	139.9	0	854.0	7.615	140.9	0
S-32	FWH4	V-2	129.4	3.416	219.3	0	147.7	3.446	215.2	0
S-33	V-1	DA1	4.5	0.350	138.9	0.920	7.4	0.360	139.9	0.913
S-35	SP-4	FWH_DW2	5.3	7.269	139.9	0	849.5	7.615	140.9	0
S-37	M-1	Steam Line Pipe	959.5	6.481	297.4	1	1144.1	6.733	298.9	1
S-38	V-3	FWH1	30.2	0.035	66.5	0	29.8	0.033	65.4	0
S-39	CAS_IN	SP-9	860.8	3.500	210.0	0	860.8	3.500	195.0	0
S-39a	SP-9	DIV_CAS	859.4	3.500	210.0	0	11.2	3.500	195.0	0
S-39b	SP-9	M-9	1.4	3.500	210.0	0	849.6	3.500	195.0	0
S-4	V-5	M-6	2.1	0.527	199.9	1	54.5	0.423	194.6	1
S-40	M-9	CAS_OUT	860.8	3.500	179.7	0	860.8	3.500	194.7	0
S-40a	DIV_CAS	M-9	859.4	3.500	179.7	0	11.2	3.500	171.5	0
S-41	M-5	FWH3	797.1	7.029	203.1	0	939.2	7.462	191.2	0
S-43	V-2	FWH3	129.4	2.500	219.3	0	147.7	2.500	215.3	0
S-44	SP-6	V-8	0.5	6.381	296.2	1	42.3	6.598	297.4	1
S-45	FWH3	M-3	797.1	6.862	221.1	0	939.2	7.258	217.9	0
S-46	FWH3	PUMP-3	162.4	2.463	208.6	0	204.9	2.392	201.0	0
S-47	FWH1	V-4	73.1	0.033	32.0	0	70.9	0.031	31.9	0
S-49	FWH_DW1	PUMP-4	3.2	0.519	136.0	0	145.1	0.409	142.6	0
S-50	DIV_PFC	M-2	691.0	0.457	135.5	0	7.1	0.531	133.0	0
S-51	FWH_DW1	M-2	17.4	0.528	153.2	0	694.4	0.444	134.4	0
S-52	SP-6	V-9	0.6	6.381	296.2	1	48.3	6.598	297.4	1
S-53	SP-3	DIV_PFC	691.0	0.528	89.0	0	7.1	0.531	87.9	0
S-54	SP-3	FWH_DW1	17.4	0.528	89.0	0	694.4	0.531	87.9	0
S-55	SP-1	V-5	2.1	6.381	296.2	1	54.5	6.598	297.4	1
S-56	PUMP-3	M-3	162.4	6.780	209.7	0	204.9	7.096	202.1	0
S-57	V-11	FWH4	92.8	3.650	245.0	0.058	103.0	3.650	245.0	0.139
S-58	HX_REHEAT	V-11	92.8	6.381	265.4	0	103.0	6.598	281.8	0.037
S-59	SP-4	VV	710.9	7.269	139.9	0	4.5	7.615	140.9	0
S-60	FWH_DW2	M-4	5.3	7.269	188.3	0	849.5	7.592	165.4	0
S-61	PUMP-A1	M-4	81.0	7.190	185.2	0	85.2	7.576	185.0	0
S-62	M-4	SP-5	797.1	7.178	169.9	0	939.2	7.576	167.3	0
S-63	SP-5	DIV_CAS	786.0	7.178	169.9	0	10.0	7.576	167.3	0

S-64	SP-5	FWH_DW3	11.1	7.178	169.9	0	929.2	7.576	167.3	0
S-65	DIV_CAS	M-5	786.0	7.029	203.2	0	10.0	7.576	193.5	0
S-66	FWH_DW3	M-5	11.1	7.178	197.5	0	929.2	7.462	191.1	0
S-67	M-6	FWH_DW1	3.2	0.519	153.2	0.680	145.1	0.423	145.6	0.441
S-68	V-6	M-6	0.5	1.168	144.3	0	42.3	0.423	145.6	0.048
S-69	V-7	M-6	0.6	0.519	153.2	0.041	48.3	0.423	145.6	0.099
S-70	FWH_DW2	V-6	0.5	1.168	144.3	0	42.3	0.881	169.0	0
S-71	FWH_DW3	V-7	0.6	1.449	173.0	0	48.3	1.507	193.7	0
S-72	V-8	FWH_DW2	0.5	1.168	214.8	1	42.3	0.905	206.4	1
S-73	V-9	FWH_DW3	0.6	1.449	220.8	1	48.3	1.595	221.6	1
S-74	HX_REHEAT	ST4	708.4	1.049	268.0	1	701.5	1.041	270.1	1
S-75	ST6	CND1	635.4	0.005	32.9	0.846	630.7	0.005	32.9	0.848
S-78	ST4	PI-3	30.2	0.084	94.8	0.944	29.8	0.083	94.6	0.946
S-79	ST5	PI-4	42.9	0.034	71.9	0.909	41.1	0.034	71.7	0.910
S-82	SP-2	BZ OTSG	810.7	6.581	238.5	0	8.4	6.833	237.7	0
S-83	SP-2	MS HCSG	148.8	6.581	238.5	0	1135.8	6.833	237.7	0
S-84	BZ OTSG	M-1	810.7	6.481	299.0	1	8.4	6.833	289.9	1
S-85	MS HCSG	M-1	148.8	6.579	290.3	1	1135.8	6.733	299.0	1
S-86	ST1	PI-1	36.6	3.510	242.7	0.969	44.7	3.581	243.9	0.964
S-87	ST2	PI-2	33.0	2.500	223.9	0.941	57.2	2.494	223.8	0.935
S-88	ST3	V-1	4.5	1.100	184.1	0.889	7.4	1.091	183.7	0.884
S-89	V-10	DA1	711.6	0.350	135.9	0	846.6	0.360	135.8	0
S-9	FWH2	V-3	30.2	0.080	66.5	0	29.8	0.076	65.4	0
S-90	Steam Line Pipe	SP-6	959.5	6.381	296.2	1	1144.1	6.598	297.4	1
S-91	FWH LINE PIPE	SP-2	959.5	6.581	238.5	0	1144.1	6.833	237.7	0
S-92	PI-1	FWH4	36.6	3.464	242.0	0.969	44.7	3.515	242.8	0.964
S-93	PI-2	FWH3	33.0	2.500	223.9	0.941	57.2	2.494	223.8	0.935
S-94	PI-3	FWH2	30.2	0.082	94.0	0.945	29.8	0.081	93.8	0.946
S-95	PI-4	FWH1	42.9	0.033	71.2	0.909	41.1	0.033	71.1	0.911
S-96	PUMP-4	M-2	3.2	0.520	136.0	0	145.1	0.490	142.7	0
S-A1	MSEP1	PUMP-A1	81.0	1.100	184.1	0	85.2	1.091	183.7	0

where $W_{Rankine\ pump\ i}$ is the power consumed by the i-th pump ($i = 1..5$) in the considered PCS circuit. The electric power (W_e) was defined as:

$$W_e = W_{gross} - \sum_i W_{pump_i} \qquad (3)$$

where $W_{pump\ i}$ is the power consumed by the i-th pumping device in the primary, secondary and tertiary loops, which apart from the 5 pumps in the PCS include also pumps specified in Table 4, which are not considered in our GC model.

Table 4. Power (in MW) consumed by pumps in the primary and tertiary loops not included in our model [17]

Loop	PULSE	DWELL
BB BZ	4 × 3.39	4 × 3.39
BB FW	2 × 2.1	2 × 2.1
DIV PFCs	5.99	5.99
VV	2 × 1.574	2 × 1.574
DIV Cas	0.15	0.15
Condenser cooling water	13.9	13.9
Molten salt	7	14.1
Total	47.95	55.05

The respective gross, cycle and electric efficiencies of were obtained from:

$$\eta_{gross} = W_{gross} / Q_{Reactor}, \qquad (4a)$$

$$\eta_{cycle} = W_{cycle} / Q_{cycle}, \qquad (4b)$$

$$\eta_e = W_e / Q_{Reactor}, \qquad (4c)$$

where $Q_{Reactor}$ is the rate of heat released by the reactor heat sources (BB FW, BB BZ, DIV CAS, DIV PFCS and VV) specified in Table 1, whereas

$$Q_{cycle} = Q_{BZ\ OTSG,cy} + Q_{MS\_HCSG} + Q_{DIV\_CAS,cy} +$$
$$+ Q_{VV,cy} + Q_{DIV\_PFC,cy} \qquad (4d)$$

is the thermal power absorbed by feed water or steam at the cold side of the HXs: BZ OTSG, DIV_CAS, DIV_PFC, VV and MS_HCSG in the considered Rankine cycle. It should be noted that the gross efficiency (η_{gross}) is referred to fusion power only, thus it is expected to be much greater than 100% during dwell, when most of thermal power is provided to the PCS circuit from the ESS. We calculated power and efficiencies of the PCS for the pulse phase, for the dwell phase and averaged for the whole operation scenario of the cycle (pulse + dwell). The last ones were computed as the weighted average with $t_{pulse} = 120$ min and $t_{dwell} = 10$ min serving as weights.

3. Results

The values of the optimized operating parameters of the considered PCS circuit, for both the pulse and dwell phases, are gathered in Table 3, whereas the respective

T-s diagrams are shown in Fig. 2. The thermal power supplied to the Rankine cycle from different heat sources and the results of cycle power and efficiency evaluation are compiled in Table 5.

It can be noticed in Fig. 1 that the feedwater flow around the DIV_PFC, VV and DIV_CAS HXs was being split into the main flow and the by-pass flow through the HXs FWH_DW1, FWH_DW2 and FWH_DW3, respectively. During the dwell phase, when the thermal power supplied to the HXs DIV_PFC, VV and DIV_CAS HXs is significantly reduced, the main flow is also strongly decreased accordingly (streams S-53, S-59 and S-63), in order to reduce the temperature fluctuations $\Delta T = |T_{pulse} - T_{dwell}|$ in these HXs. Power reduction of the DIV PFC, VV and DIV CAS heat sources is compensated by significant increase of thermal power supplied to HXs FWH_DW1, FWH_DW2 and FWH_DW3, respectively, which was achieved by considerable increase of live steam mass flow taken from splitters SP-1 and SP-6 (streams S-55, S-44 and S5-2).

During the whole operation period (pulse + dwell) the water / steam parameters in all the PCS components are within the reasonable range, while the temperature fluctuations $\Delta T = |T_{pulse} - T_{dwell}|$ in all of the PCS components are very small (the highest value of
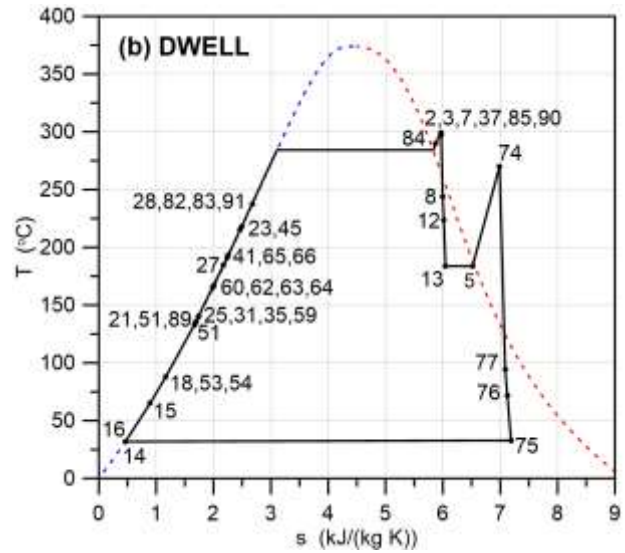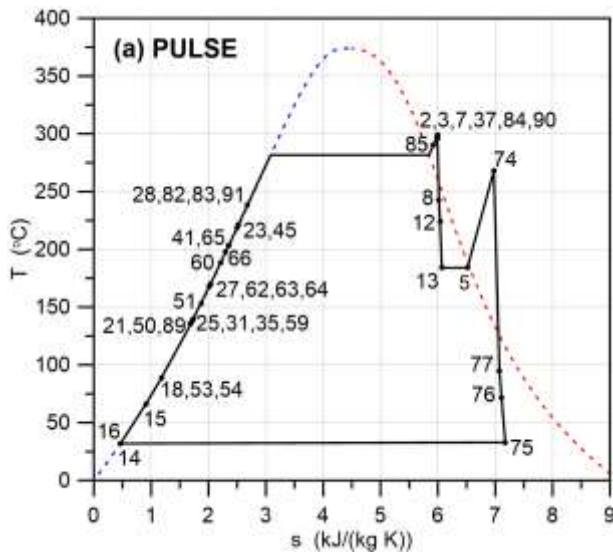

Fig. 2. T-s diagram for the considered PCS cycle during the pulse phase (a), and during the dwell period (b).

Table 5. Results of the power and efficiency calculations

Description	PULSE	DWELL	
$Q_{MS\,HCSG,cy}$ (MW)	265.96	2068.17	
$Q_{BZ\,OTSG,cy}$ (MW)	1482.96	14.83	
$Q_{DIV\_CAS,cy}$ (MW)	115.23	1.15	
$Q_{VV,cy}$ (MW)	86.00	0.86	
$Q_{DIV\,PFC,cy}$ (MW)	136.00	1.37	
Q_{cycle} (MW)	2086.16	2086.38	
$Q_{Reactor}$ (MW)	2260.00	22.60	
W_{t1} (MW)	242.72	252.71	
W_{t2} (MW)	539.83	535.82	
W_{pump1} (MW)	0.61	0.60	
W_{pump2} (MW)	6.73	8.43	
W_{pump3} (MW)	1.11	1.44	
W_{pump4} (MW)	0.00	0.02	
W_{pumpA1} (MW)	0.70	0.79	
Description	PULSE	DWELL	Average
W_{gross} (MW)	766.90	772.76	767.35
W_{cycle} (MW)	773.39	777.26	773.69
W_e (MW)	709.80	706.43	709.54
η_{gross} (%)	33.93	3419.29	36.75
η_{cycle} (%)	37.07	37.25	37.09
η_e (%)	31.41	3125.80	33.98

ΔT =24.8 °C is observed in stream S-70). The smallest value of the steam quality in turbines equal to 0.846 (stream S-75 at the outlet of the LP turbine during the pulse phase) is also acceptable. These are optimistic results, which may imply the potential operational feasibility of the considered PCS. The power of the considered PCS circuit remain at the almost constant level during the whole operation scenario.

4. Summary, conclusions and perspectives

We have created the detailed convergent GC model of the fully mature PCS configuration for the EU-DEMO option WCLL BB with IHTS+ESS (based on the 2018

EU-DEMO reference). The model was used to simulate operation of the EU-DEMO PCS during the plasma burn and during the dwell phase. The operating parameters of the circuit were optimized to minimize the temperature oscillations $\Delta T = |T_{pulse} - T_{dwell}|$ in all the circuit components, which occur due to the pulsation of thermal power of the EU-DEMO cold sources of Divertor and Vacuum Vessel whose HXs are integrated in PCS itself. We managed to reduce the maximum value of ΔT down to about 25 ℃ which is an encouraging result, which may indicate that the thermal stresses during the PCS operation should remain at the acceptable level. It was demonstrated, that the proposed PCS circuit allows almost constant production of electricity during both plasma pulse and dwell phases with the average gross/electric power of about 767 /710 MW and with the average gross/electric efficiency of about 37/34%. It should be noted that the DEMO plant final net power and the related net plant electrical efficiency will be lower than the W_e and η_e values mentioned above, since the power consumption of the DEMO's auxiliary systems, e.g. those ones required for plasma heating and current drive, magnet system, cryogenic plant, vacuum pumps, etc., have not been taken into account to evaluate the Balance of Plant efficiency.

It should also be mentioned that ESS required by the proposed PCS concept is very huge (2 MS tanks with the volume of about 11 000 m^3 per tank) [17,18] This is the main drawback of the proposed solution, which implies also an increase on the cost of the plant. Further research is carried out in parallel on more direct coupling option between the PHTS and PCS (without IHTS and with small ESS) [20].

Acknowledgments

References

[1] A.J.H. Donné, W. Morris, European Research Roadmap to the Realisation of Fusion Energy, Nov. 2018, ISBN 978-3-00-061152-0.

[2] G. Federici, et al., DEMO design activity in Europe: Progress and updates, Fus. Eng. Des. 136 (2018) 729-741.

[3] G. Federici, et al., Overview of the DEMO staged design approach in Europe, Nucl. Fusion 59 (2019) Art. No. 066013.

[4] C. Bachmann, et al., Key design integration issues addressed in the EU DEMO pre-concept design phase, Fus. Eng. Des. 156 (2020) Art. No. 111595.

[5] L. Barucca, et al., Status of EU DEMO heat transport and power conversion systems, Fusion Eng. Des. 136 (2018) 1557–1566.

[6] S. Ciattaglia, et al., EU DEMO safety and balance of plant design and operating requirements. Issues and possible solutions, Fus. Eng. Des. 146 (2019) 2184-2188.

[7] F.A. Hernandez, et al., Overview of the HCPB Research Activities in EUROfusion, IEEE Trans. Plasma Sci. 46 (2018) 2247-2261.

[8] I. Moscato, et al., Progress in the design development of EU DEMO helium-cooled pebble bed primary heat transfer system, Fus. Eng. Des. 146 (2019) 2416-2420.

[9] E. Martelli, et al., Study of EU DEMO WCLL breeding blanket and primary heat transfer system integration, Fus. Eng. Des. 136 (2018) 828-833.

[10] A. Del Nevo, et al., Recent progress in developing a feasible and integrated conceptual design of the WCLL BB in EUROfusion project, Fus. Eng. Des. 146 (2019) 1805-1809.

[11] E. Bubelis, W. Hering, S. Perez-Martin, Industry supported improved design of DEMO BoP for HCPB BB concept with energy storage system, Fus. Eng. Des. 146 (2019) 2334–2337.

[12] L. Malinowski, M. Lewandowska, E. Bubelis, W. Hering Design and analysis of the secondary circuit of the DEMO fusion power plant for the HCPB BB option without the energy storage system and with the auxiliary boiler, Fus. Eng. Des. 160 (2020) 112003.

[13] A. Bender, S. Gil Pascual, H. Sommer, DEMO Balance of Plant – Evaluation and Approximation of a minimal ESS for a Direct-Coupling Configuration, Technical Note December 2018. KAH Doc. No. BoP-0011_DN (unpublished).

[14] L. Malinowski, M. Lewandowska, F. Giannetti, Analysis of the secondary circuit of the DEMO fusion power plant using GateCycle, Fus. Eng. Des. 124 (2017) 1237–1240.

[15] L. Malinowski, M. Lewandowska, F. Giannetti, Design and analysis of a new configuration of secondary circuit of the EU-DEMO fusion power plant using GateCycle, Fus. Eng. Des. 136 (2018) 1149–1152.

[16] L. Malinowski, M. Lewandowska, F. Giannetti, Design and analysis of the improved configuration of the secondary circuit for the EU-DEMO power plant, Fus. Eng. Des. 146 (2019) 1035-1038.

[17] F. Giannetti, A. Del Nevo, G. Padula, L. Ferroni, DEMO 16 sectors BoP - Gate Cycle Analysis to support WCLL BB PCS preliminary design in plant configuration with IHTS+ESS, Final report for the task BOP-2.2-T017-D001 (2019) https://idm.euro-usion.org/?uid=2MU6KN .

[18] P. Lorusso, E. Martelli, A. Del Nevo, V. Narcisi, F. Giannetti, WCLL BB DEMO Configuration with IHTS+ESS: BB/DIV/VV PHTS, IHTS, ESS and Power Conversion System (PCS) Preliminary Design (DDD). Final report for the task BOP-2.2-T006-D003 (2020) https://idm.euro-usion.org/?uid=2MZA8S .

[19] M. Lewandowska, L. Malinowski, DEMO WCLL BB

BOP (Indirect Coupling Option) - PCS Gate Cycle Analysis. Final report for the task BOP-2.2-T032-D001 (2020) https://idm.euro-usion.org/?uid=2MQVWE with the attachment: GateCycle Report - Model PULSE-P1-9-DWELL Case PULSE-Creation Time 5_22_2020 21 16 17.docx

[20] L. Barucca, et al., Pre-conceptual design of EU DEMO balance of plant systems: objectives and challenges, submitted to Fusion Eng. Des.